Scientific report

The visit was intended on strengthening the established collaboration between the groups lead by Prof. Baumberg at Cambridge University and Prof. Savvidis at FORTH, Crete on the development and study of new class of strongly coupled semiconductor microcavities in which the strength of polariton-polariton interactions can be tuned by controlled electronic tunneling in asymmetric double quantum wells (ADQWs). Application of an electric field to the structure, allows the alignment of electronic levels of neighboring QWs into resonance where the spatially direct and indirect excitons become coupled. As a result the indirect exciton transition acquires oscillator strength and both excitons couple to light forming symmetric and asymmetric polariton states. Furthermore due to tunneling of electrons polaritons in these structures possess enhanced dipole moments in the growth direction. The later can be exploited to enhance polariton-polariton interactions responsible for relaxation and scattering of polaritons making these structures very promising for studies of nonlinearities and the demonstration of many types of optoelectronic devices. In the following, a short description of the progress performed during these six months is given in the field of the asymmetric QWs.

Sample description-Fabrication methods

The microcavities used in the experiments consist of a n-doped bottom DBR and a p-doped top DBR, separated by an undoped cavity layer as shown in fig.1b. The active region is made up of pairs of QWs spaced by a thin tunneling barrier of a few nanometers in width. The InGaAs QWs in each pair have slightly different In content, so at flatband conditions the ground energy levels in each QW are separated, activating only the DX transition in the left QW. Reverse bias voltage brings the two levels into resonance (fig.1a), so that the tunneling rate of electrons into the right QW and back enhances the IX coupling to the polariton modes and leading to the formation of dipolaritons with out-of-plane dipole moment, fig.1d.

The samples are grown by molecular beam epitaxy on highly n-doped GaAs (001) substrates. The p-i-n microcavity structure consists of a highly n-doped lower DBR (21 GaAs/AlAs periods) and a highly p-doped upper DBR (17 GaAs/AlAs periods). The 5λ/2 undoped cavity contains 4 sets asymmetric double QWs (ADQWs) of $In_{0.1}Ga_{0.9}As$/GaAs/ $In_{0.08}Ga_{0.92}As$ (10nm/L_B/10nm), placed at the antinodes of the electric field. Three sample wafers with barrier width L_B of 4nm, 7nm and 20nm are fabricated to access different coupling strengths. Cylindrical mesas of 200, 350 and 500μm diameter are processed into the samples using BCl_3/Cl_2 reactive ion etching. Ti/Pt p-type contacts were formed in a ring-shaped geometry at the edge of the mesas after an etching ohmic recess step to reduce the series resistance of the top DBR bringing the contact closer to the cavity.

Finally, the n-type (Au/Ge) ohmic contact was back-side evaporated. The ohmic contacts were activated by rapid thermal annealing at 420 ^{o}C [1].

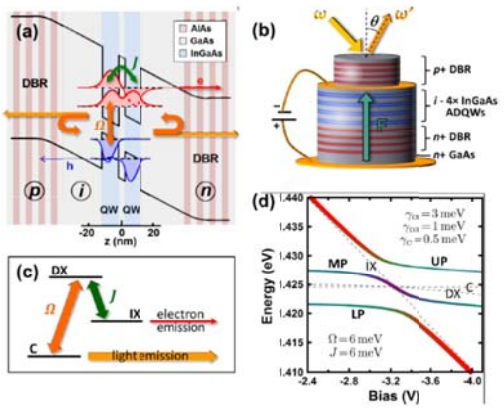

Figure 1: (a) Schematic band structure at tunneling resonance, surrounded by doped mirrors. (b) Structure of electrically-contacted mesa. (c) Three level Λ-scheme coupling cavity (C), direct (DX) and indirect (IX) modes by classical intense laser pump Ω and quantum tunneling J. (Coupling of IX (red), DX (green) and cavity mode (blue) produces the three dipolariton modes LP, MP, UP. The thickness of the simulated lines represents the linewidth of the modes.

Optical Characterization

Optical measurements are performed in a temperature stabilized continuous-flow liquid helium cryostat at T~20K. Each mesa is excited non-resonantly at the first high energy minimum of the microcavity reflectivity by a Ti-sapphire laser. The whole set up is shown in fig.2.

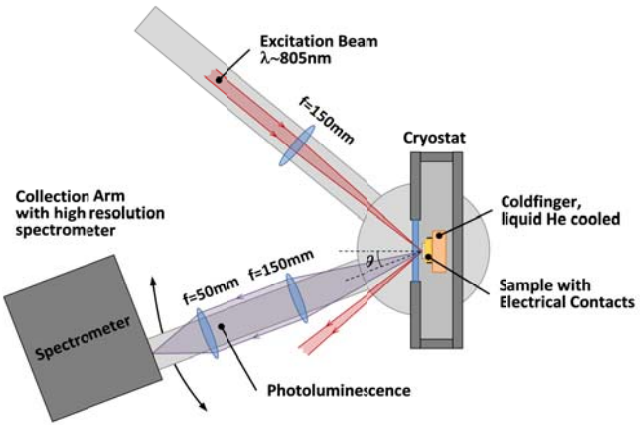

Figure 2: Angle-resolved photoluminescence (PL) set up with high angle non-resonant excitation beam. The PL is collected with a high resolution spectrometer on a goniometer arm.

Experimental results

The design of the microcavity enables mixing of direct (DX) and indirect (IX) exciton through electron tunneling, controlled by a static electric field. The resonator ensures strong coupling of the DX to the light field C, so that three clearly split modes appear in the spectrum under resonant bias as shown in fig. for a mesa with L_B=4nm. As it is shown in fig.3, at normal incidence (a,c) the narrow cavity mode is detuned 10 meV below the excitons at zero bias.

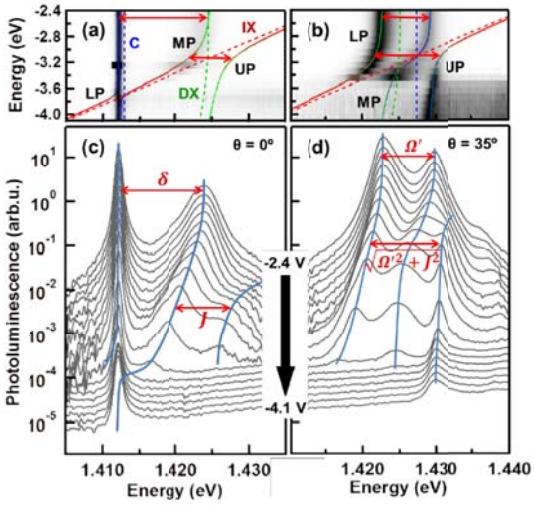

Figure 3: PL spectra with bias voltage for (a,c) the off resonant cavity and (b,d) close to the resonance for a mesa with $L_B = 4nm$. Polariton lines LP, MP and UP are fits to the coupled oscillator model, while the dashed lines show the uncoupled modes: C (blue), DX (green) and IX (red).

As the reverse bias increases more, we have a transition in which the low energy exciton transforms from DX to IX, tracking the electron's location from left to right QW and at -3.2V there is an anticrossing between the MP and UP branches.

The situation changes at high angle (b,d) where the cavity mode is resonant with the indirect exciton. At low bias voltage IX is far detuned and the system behaves as a single QW microcavity with direct excitons only, producing a detuned splitting $\Omega' = \sqrt{\Omega^2 + \delta^2}$ where $\delta(U,\theta)$ is the detuning of DX below C at each bias and angle. Resonance between DX, IX and the C is reached at U= -3.2V, as we can see clearly the existence of three distinct polariton branches. In this case the total anticrossing shown at figures (b,d)

is $S=\sqrt{\Omega'^2+J^2}$. The eigenvectors at resonance ($\omega_C=\omega_{IX}=\omega_{DX}+\delta$) can be easily shown that are given from the following equations, by diagonalizing a three mode Hamiltonian.

$$\left|MP\right\rangle=\frac{\Omega\left|IX\right\rangle-J\left|C\right\rangle}{\sqrt{\Omega^2+J^2}} \tag{0.1}$$

$$\left|\begin{matrix}UP\\LP\end{matrix}\right\rangle=\frac{J\left|IX\right\rangle+\Omega\left|C\right\rangle-\left(\delta\pm S\right)\left|DX\right\rangle}{\sqrt{2S\left(S\pm\delta\right)}} \tag{0.2}$$

Surprisingly, while the MP branch has no DX admixture at resonance, it is clearly visible in emission through the tunneling interaction with the cavity photon and almost strong as the other polaritons. The absence of DX in the MP is confirmed in fig.4b, which shows the composition of each polariton modes versus bias. By increasing the electric field the MP turns from an ordinary DX-polariton to a pure dipolariton at resonance, equation (1.1), with the electron and hole located in different QWs and possessing a static dipole moment oriented perpendicularly to the QW plane. The LP branch could be of particular interest for condensation experiments because of the intensive tuning possibilities of the dipolaritons with cavity detuning and bias voltage, as the bottom graph in fig.4b demonstrates.

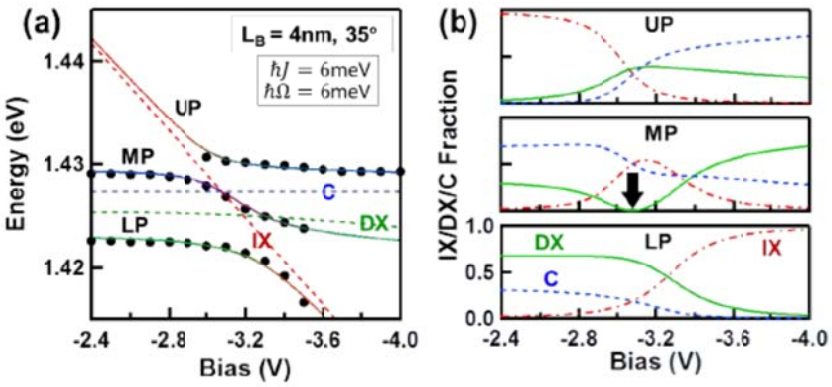

Figure 4: Bias dependent polariton modes observed in PL for $L_B=4nm$. The solid lines are fits using coupled oscillator model. (b) Bias dependence of the polariton composition as computed from the fits to (a). Black arrow for MP marks the position of the pure dipolariton.

Influence of the tunneling barrier width

To study the influence of the tunneling rate J to dipolaritons modes three wafers with barrier widths of 4nm, 7nm and 20nm were grown as described before. PL experiments show the dependence of the three polariton modes on this tunnel coupling (fig.5 a-c).

Different bias voltages were required for mesas to bring DX and IX into resonance, overcoming the intrinsic p-i-n electric field and the fact that mesas with larger tunneling barrier require higher fields to make the electron levels of the two QWs degenerate. Also, because of the variation of the cavity mode energy at different mesas, data are recorded at the appropriate angles to bring in resonance the cavity mode with excitons. To extract the values for Ω, J, and the bare modes $|IX\rangle, |DX\rangle, |C\rangle$ the data are fitted with a coupled oscillator model.

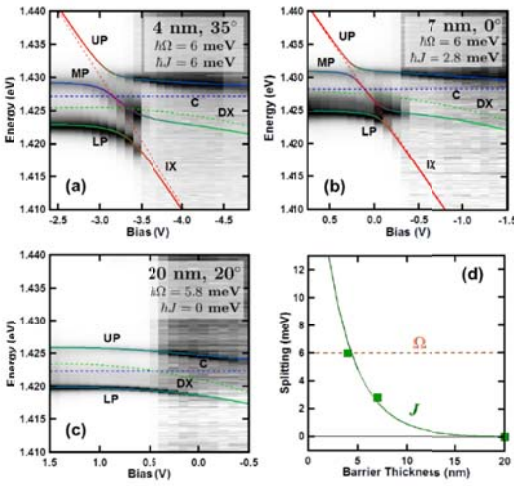

Figure 5: Bias dependent polariton modes observed in PL (log intensity scale) for samples with LB of (a) 4nm, (b) 7nm and (c) 20nm. Solid coloured lines are fits to the coupled oscillator model with line colour reflecting the composition of each polariton mode (red: IX, green: DX, blue: cavity). (d) Tunnel splitting J versus barrier thickness, showing match between theoretical fit (solid line) and J extracted from data (squares). Dashed orange line is measured vacuum Rabi splitting Ω of the microcavity.

In all three samples the PL disappears rapidly beyond a certain negative bias voltage. This behavior can be attributed tto the reduction of the triangular barrier on the right side of the ADQW which becomes small enough so that electrons can tunnel out of the system within the 3-5ps polariton radiative lifetime, as seen previously in reflectivity [2]. The results in fig.5 a-c clearly show that a large tunneling rate is necessary to optically couple the IX to the active mode. For larger barrier widths $L_B \geq 20nm$ the system behaves like an ordinary DX-polariton microcavity with weak electric tuning and the dipolariton modes disappear. In fact the optimum condition for pure dipolaritons is $\Omega = J$.

By fitting the experimental data with the coupled oscillator model we are able to extract the bare tunneling rate *J* versus barrier thickness for the three different mesas, fig.5d. for the three mesas. These data points (green squares) nearly match the tunneling splitting calculated from parameter-free solutions of the Schrodinger equation for this asymmetric double QW system with electric field [2], showing the expected exponential decrease in splitting with increased barrier width.

Tunneling control with angle and bias

Fig.6 shows measurements of the dipolariton modes in the parameter space of bias voltage *U* and cavity angle θ. Each spectrum has been normalized to its maximum value to better reveal the polariton modes. Fig.6a shows the bias-dependence by increasing collection angles θ, which shifts the cavity mode in energy through the exciton resonance, following the well known quadratic behavior. The solid lines (described as in fig.3) are fits to the data using only the cavity energy as a free parameter while the rest parameters remain constant. At small or large collection angles the cavity mode is far detuned and the dynamics of the system are controlled by the tunneling resonance of the DX with the IX. Exact resonance of all three modes is obtained at $\theta = 30^{o}$, where the splittings LP-MP and MP-UP become equal.

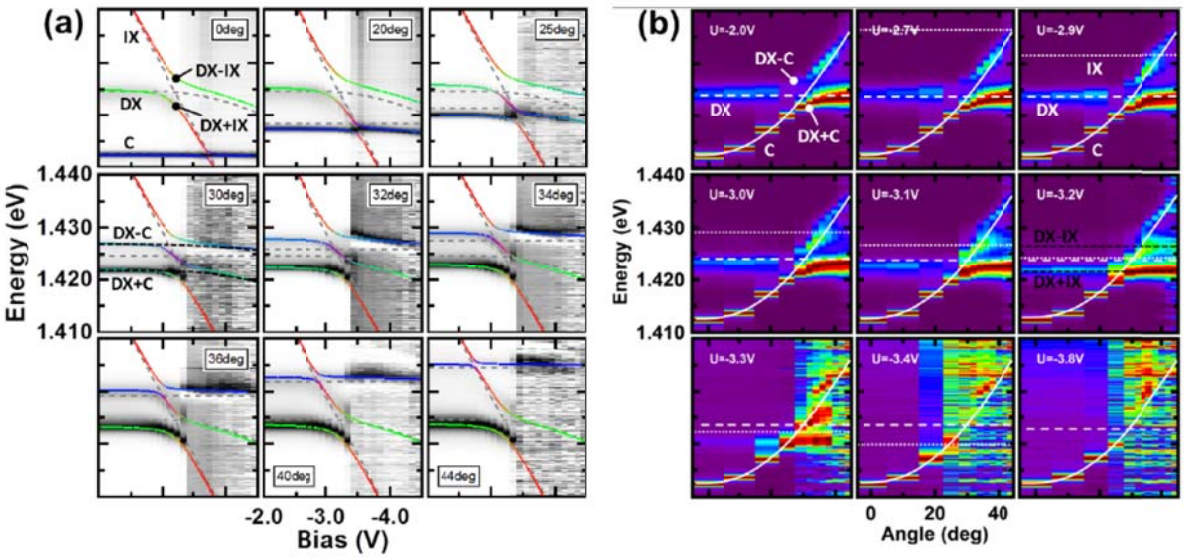

Figure6: (a) Bias tuning of the mode coupling measured in PL at different angles. In the top left graph the tunneling splitting $\hbar J = 6\,meV$ between the coupled excitons in visible. (b) Same PL data set as in (a), presented as angle tuning of the modes at different bias values. The white lines refer to C (solid), DX (dashed) and IX (dotted). In the top left graph $\hbar\Omega = 6$ between DX and C.

Fig.6b presents the same data in a different way. This time the DX (dashed) and especially the IX mode (dotted) red-shift with increasing bias voltage, whereas the parabolic dispersion of C (solid line) remains unchanged throughout all nine graphs. The graphs reveal the presence of the three dipolariton modes *at* $U=-3.2V$ *and* $U=-3.3V$ and demonstrates again how the PL is lost at higher electric fields, independently of the angle θ. For condensation experiments of dipolaritons, the region of positive DX detuning ($\theta=25^o, U=-3.3V$) is particularly interesting because of the large optical-dipole coupling strength.

Finally, fig7. presents sets of spectra that show how tunneling can be switched on or off with bias voltage and cavity detuning. In the case of bias switching (a,b) the intensity of the PL drops strongly. In figs. 4,5a, DX and C are always close to resonance and form DX-polariton. With increasing bias voltage the IX shoots in from the high energy side to switch on the gradually the tunneling interaction. The amplitude of the spectrum **B** with tunneling ("on"-state) is only 1/10 of the "off" state **A** (fig7.b). On contrary, with angle-switching (c,d) the uncoupled modes in fig 7.c show the two exciton modes in resonance producing coupled excitons $\left|\begin{matrix}X_A\\X_B\end{matrix}\right\rangle=\frac{1}{\sqrt{2}}\left(\left|DX\right\rangle\mp\left|IX\right\rangle\right)$ (black dotted lines), as can be seen by the peaks far away from resonance which are space s by the tunneling interaction $\hbar J=6\,\text{meV}$ (tunneling "on" all the time). As the cavity couples into the system from the low energy side the PL signal strongly increases (Ω switches "on") and the three familiar dipolariton peaks reappear in spectrum.

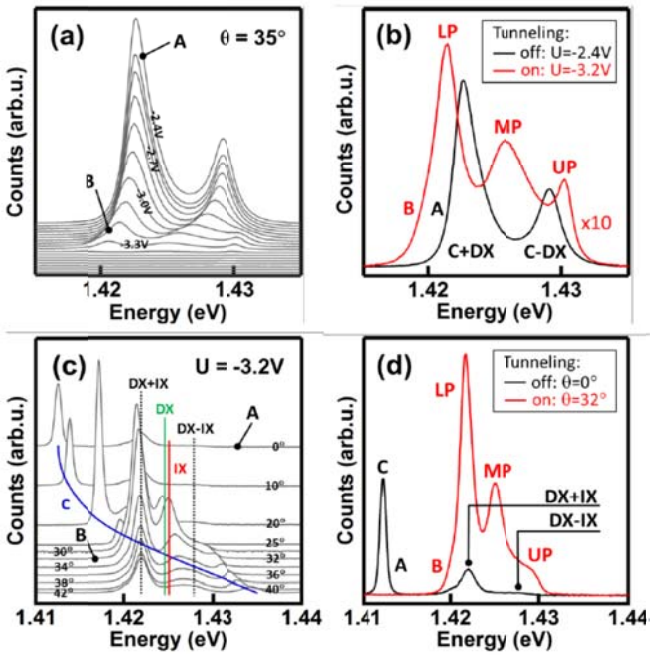

*Figure 7: tunneling control with bias voltage and angle. (a) Bias dependence of PL at 35°. (b) At low voltage $U = -2.4V$ the microcavity produces standard DX-polaritons (**A**) while at resonance $U = -3.2V$ tunneling is switched on and three equidistant peaks appear (**B**). (c) Angle dependence of the tunneling coupling. (d) sSpectrum with off-resonant cavity, when the tunneling coupling slits the excitons into asymmetric and antisymmetric state (**A**) and when tunneling couples all the three modes to form dipolaritons (**B**).*

Limitations of the sample

Over the course of many PL-measurements performed on different mesas, several limitations of the sample have become apparent. Most significantly the PL signal from two of dipolariton modes vanishes at bias voltages slightly higher than resonance, leaving only weak emission from the most cavity like mode. This observation is linked to the electron being able to tunnel through the triangular barrier on the right side of the ADQW system at a rate faster than the Rabi cycle time [3] (fig1a). This loss of PL signal depends strongly on the excitation power (fig.8a) but only insignificantly on the tunneling barrier width L_B and matches with the onset of strong photocurrent, as seen from resonant excitation experiments on these samples. As fig. 8a shows, the resonance point shifts exponentially to higher voltages with increasing pump power. This suggests a reduced electric field inside the cavity which can be attributed to the charging of the DBRs[54] with free electrons and holes that screen part of the applied voltage.

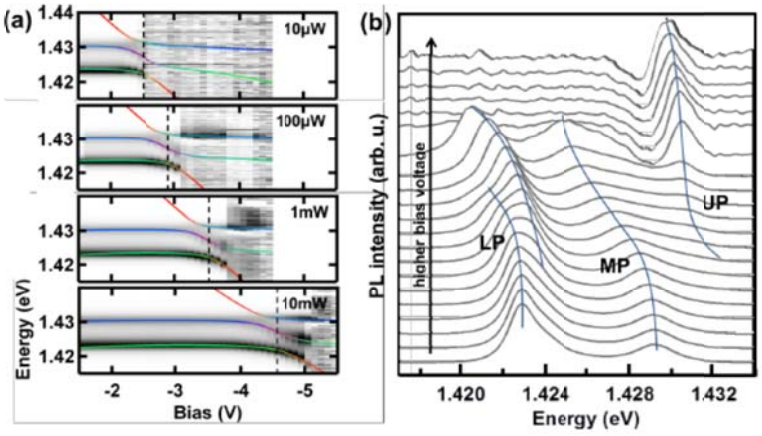

Figure 8: (a) Non-resonant excitation power dependence of the PL under bias tuning. Dashed lines mark resonant point which shifts to higher bias values for increasing pump power. (b) Level crossing of the DX as seen in PL from some mesas in bias tuning on the LP, blue lines are guides to the eye.

Furthermore the bias tuning response of the excitons becomes weaker, as seen from the diminished slope of the IX mode, which could stem from a series resistance in the DBRs.

Moreover, we found that different mesas on the same sample start tuning at different bias voltage, an observation we have no explain so far. For all the above mentioned reasons, it is not possible to relate tha applied bias voltage directly to the intracavity electric field strength *F*.

There are several ideas to improve the current sample design. The most obvious is the introduction of a 8nm wide AlAs potential barrier to both sides of the ADQW to prevent the electron from escaping the coupled QW system. Basic simulations, obtained by calculationg the electron wavefunction in the QW system under presence of a static electric field as in [2], have shown a reduction of the electron escape rate by 3-4 orders of magnitude with this AlAs barrier. Based on these simulations a new sample was grown with L_B = 7nm, and diodes fabricated following the same processing procedure described at the beginning.

1. *S.I. Tsintzos, P.G. Savvidis, G. Deligeorgis, Z. Hatzopoulos, N.T. Pelekanos, "Room temperature GaAs exciton-polariton light emitting diode", Appl. Phys. Lett., 94, 071109, 2009.*

2. *G. Christmann, A. Askitopoulos, G. Deligeorgis, Z. Hatzopoulos, S.I Tsintzos, P.G Savvidis, J.J Baumberg, "Oriented polaritons in strongly-coupled assymetric double quantum well microcavities", Appl. Phys. Lett., 98, 081111, 2011.*

3. *G. Christmann, C. Coulson, J. J. Baumberg, N.T. Pelekanos, Z. Hatzopoulos, S.I. Tsintzos, P.G. Savvidis, "Control of polariton scattering in resonant-tunneling double-quantum-well semiconductor microcavities", Phys. Rev. B 82, 113308 (2010).*

Joint Publications

The results of this fruitful collaboration between our groups are reflected by the large number of high impact publications listed below:

1. "Controlling quantum tunnelling with light", P. Cristofolini, G. Christmann, S. I. Tsintzos, G Deligeorgis, G Konstantinidis, Z. Hatzopoulos, P.G. Savvidis and J. J. Baumberg, to be submitted to Science (2011)

2. "Ultralow threshold crossover from strong to weak coupling lasing in a high-Q planar GaAs microcavity", P. Tsotsis, P. S. Eldridge, T. Gao, S. I. Tsintzos, Z. Hatzopoulos, and P. G. Savvidis, Under review in New Journal of Physics (2011)

3. “Polariton ring condensates and sunflower ripples in an expanding quantum liquid”, G. Christmann, G. Tosi, N.G. Berlo, P. Tsotsis, P. Eldridge, Z. Hatzopoulos, P.G. Savvidis and J. J. Baumberg, submitted to PRL (2011)

4. “Sculpting oscillators with light within a nonlinear quantum fluid”, G. Tosi, G. Christmann, N.G. Berloff, P. Tsotsis, T. Gao, Z. Hatzopoulos, P.G. Savvidis, J.J. Baumberg, 10.1038/NPHYS2182, Nature Physics (2011)

5. “Optically-induced vortex lattices in a semiconductor quantum fluid”, G. Tosi, G. Christmann, N.G. Berloff, P. Tsotsis, T. Gao, Z. Hatzopoulos, P.G. Savvidis, J.J. Baumberg, in preparation for Nature Photonics